RAI Volume 3, Chapter 2.2.1.4.2, First Set, Number 1:

> Clarify the technical basis for the amount of water entering the waste package for the human intrusion scenario. Also, provide a comparison of the amount of water estimated to enter the human intruded waste package with the amount estimated to enter waste packages that have patch failures.
>
> Basis: The SAR implies that the 'only' water that enters a waste package that is breached due to a human intrusion event is the water that enters the borehole (i.e., other seepage water does not enter the breached area caused by the intrusion). It is unclear as to why other seepage water that enters the drift could not enter the breached area of the waste package caused by the intrusion. The staff needs this information to determine compliance with 10 CFR Part 63.322.

1. RESPONSE

As detailed in SAR Section 2.4.3.1.2, the unsaturated zone borehole transport pathway in the human intrusion scenario is conceptualized to be an uncased borehole that undergoes natural degradation processes (including erosion and seismic events), resulting in rubble infill and wall rock collapse shortly after it is drilled. The use of the percolation flux at the base of the Paintbrush non-welded hydrogeologic (PTn) unit is used to determine the volumetric flow rate of water through the intruded waste package and is considered to be representative of steady-state conditions consistent with the conceptualization of the degraded borehole. The percolation flux at the base of the PTn unit is determined by the site-scale unsaturated zone flow model (SAR Section 2.3.2.1).

The only water entering the intruded waste package enters through a borehole along the apex (crown) of the waste package. The borehole opening in the top of the drift is expected to be directly above the opening in the intruded waste package; therefore, water dripping from the borehole in the top of the drift (e.g., percolation flux at the base of the PTn unit) is expected to intersect the waste package near or within the borehole opening. However, the assumption that the entire borehole flux enters the waste package neglects the effects of water being diverted from the borehole to the rubble material between the waste package and the drift crown. This assumption accounts for the possibility of any additional water flux from seepage dripping within the vicinity of the borehole. Adjacent seepage entering the waste package through the borehole is negligible, and is conservatively estimated at only about 3.5% of the mean water flow through the intruded waste package. Since it is likely that some of the borehole flow would be diverted around the waste package opening due to rubble infill and/or dispersal of the drips, adjacent seepage is captured within the assumption that all of the borehole flow exiting the borehole at the top of the drift is funneled into the drill patch opening in the top of the waste package.

The occurrence of an additional 3.5% of water flow through the intruded waste package will not significantly impact the mean annual dose projections for the human intrusion scenario. After the drilling intrusion event, there is an initial pulse of highly soluble, nonsorbing radionuclides, such as ^{99}Tc and ^{129}I, which dominate the maximum of the mean annual dose and account for

about 99% of the maximum median annual dose (SAR Section 2.4.3.3.1). A small increase in the water flow rate through the intruded waste package would not increase the mass of ^{99}Tc and ^{129}I released. These radionuclides have high dissolved concentration limits and thus, all of the available mass is rapidly released into the borehole. After the pulse of highly soluble, nonsorbing radionuclides has passed through the system, the long-term dose to the reasonably maximally exposed individual (RMEI) drops to approximately 0.0002 mrem, which occurs primarily from ^{242}Pu with secondary contributions from ^{135}Cs and ^{237}Np (SAR Section 2.4.3.3.1). As outlined in SAR Section 2.4.3.4.3, the inputs that have the greatest influence on the uncertainty in expected annual dose following the human intrusion event are those identified for the transport of ^{99}Tc. Thus, dose projections for the human intrusion performance assessment support a finding that there is a reasonable expectation the mean annual doses to the RMEI would be well below the individual protection standard for human intrusion (SNL 2008, Section 8.1.3.2[a]).

Section 1.1 contains a discussion of the estimation of the indirect seepage into an intruded waste package, and Section 1.2 contains a comparison of the repository average amount of water entering the intruded waste package through a borehole to the amount of water entering a waste package through a patch in a nominal scenario.

1.1 ESTIMATE OF INDIRECT SEEPAGE THROUGH AN INTRUDED WASTE PACKAGE

An estimation of the mean water flux from impinging seepage that may enter the breached area of the waste package caused by the intrusion is provided in Table 1. The amount of seepage impinging on the waste package crown that may enter the borehole opening can be approximated using the results of the experimental data used to develop and validate the flux-splitting model used in the total system performance assessment (TSPA) Engineered Barrier System (EBS) flow submodel (SAR Section 2.4.2.3.2.1.6). Splash distances and fractions for dripping onto the crown of an experimental drip shield surface are listed in Section 7.1.1 of *EBS Radionuclide Transport Abstraction* (SNL 2007).

The splash radius data (SNL 2007, Figures 7.1-1 and E-3) were used to calculate a mean splash radius for dripping on the crown of 21.8 cm for the inner cluster and 50.6 cm for the outer fringe. The inner cluster represents the radius of the bulk or cluster of splash droplets that accumulate around the impact point, and the outer fringe represents the farthest drip splashed from the impact point. The distance a splashed droplet can travel is finite, limited by the kinetic energy of a falling drop. The area is estimated using the mean splash radius of the inner cluster and outer fringe. Additionally, an estimate of the fraction of the dripping flux along the crown that may enter the test patch opening was provided (BSC 2003, Appendix B). Compiling the data for test patch 6, which occurs along the crown of the test surface, and interpolating between the dripping points over an equal area domain, the average fraction of drips entering the test patch within the splash area can be approximated. Using the post-10,000-year repository average seepage from the nominal modeling case, 9.47×10^{-2} m^3/yr (see Table 5 in response to RAI 3.2.2.1.3.6-2-010), approximately 3.57×10^{-5} m^3/yr of the seepage impinging within the splash area around the borehole was estimated to potentially enter the waste package. Table 1 contains a summary of these estimates. The indirect seepage flux is approximately 3.5% of the mean water flux through a waste package in the human intrusion scenario (1.03×10^{-3} m^3/yr).

The estimate of indirect seepage flux provides a quantitative evaluation of the basis for excluding other seepage water that enters the drift from entering the breached area of the waste package caused by the intrusion.

Table 1. Estimation of Additional Water Flux through a Borehole from Seepage

Location	Mean Splash Radius (cm)	Splash Area (m^2)	Drips into Borehole Patch (%)	Seepage in Splash Area (m^3/yr)	Seepage into Borehole Patch (m^3/yr)	Indirect Flux/ Borehole Flux (%)
Inner Cluster	21.8	0.45	2.23	1.50×10^{-3}	3.35×10^{-5}	3.26
Outer Fringe	50.6	1.12	0.13	3.78×10^{-3}	2.20×10^{-6}	0.21
TOTAL	—	1.57	—	5.29×10^{-3}	3.57×10^{-5}	3.48

Source: Spreadsheet: *Interpolation and Statistics for Percentage of Drop in Patch_v2_07_06_2009.xls*.

1.2 COMPARISON OF WATER FLUX THROUGH A INTRUDED WASTE PACKAGE WITH A NOMINAL PATCH OPENING

Table 2 compares the mean water flux through a borehole patch in the human intrusion scenario to the water flux through a patch failure in the nominal scenario. Water flux through the borehole opening in the waste package for the human intrusion scenario ranges from 4.78×10^{-4} to 2.28×10^{-3} m^3/yr based on the 5th and 95th percentile values of the distribution and has a mean value of 1.03×10^{-3} m^3/yr.

Using the post-10,000-year repository average seepage per waste package from the nominal modeling case, with a mean of 9.47×10^{-2} m^3/yr and 5th and 95th percentile values of 8.81×10^{-3} and 3.24×10^{-1} m^3/yr, respectively (see Table 5 in response to RAI 3.2.2.1.3.6-2-010), the calculated seepage flux through a single patch in the nominal scenario class varies from 1.42×10^{-4} to 5.22×10^{-3} m^3/yr based on the 5th and 95th percentile values of the seepage flux distribution and has a mean value of 1.53×10^{-3} m^3/yr. The ratio of the borehole opening (drill patch area is 0.0324 m^2) to the nominal patch area (0.02315 m^2) is approximately 1.4. The calculated seepage flux through 1.4 patches ranges from 1.99×10^{-4} to 7.30×10^{-3} m^3/yr, based on the 5th and 95th percentile values of the seepage flux distribution, and has a mean of 2.13×10^{-3} m^3/yr. The mean seepage flow through a single nominal patch is higher than the mean water flow through the human intrusion borehole. This is due to the uncertainty in the flux splitting model in the TSPA EBS flow submodel (SNL 2008, Section 6.3.6). The values in Table 2 are reported for the median value results for the flux splitting model uncertainty.

As described in Section 6.3.2.4 of *EBS Radionuclide Transport Abstraction* (SNL 2007), observations during the drip tests used as the basis for the waste package flux splitting model revealed that the primary mechanism for water entering breaches is via rivulet flow that originates from an area around the point of drip impact. Drips closest to the downhill curvature reach a critical mass and roll down the face of the waste package in the form of a rivulet. The rivulet flow area spreads out in a delta formation (i.e., the maximum spread is located on the vertical section of the waste package, and the minimum spread is located at the crown, which is

assumed to be the point of impact). Since nominal patch breaches in the waste package are randomly located, the fraction of dripping flux falling on the waste package that flows into the waste package might be expected to be proportional to the total area of waste package patches, as is the case for the waste package flow through the borehole opening in the human intrusion scenario. However, since patches are randomly located in the nominal scenario, drips that fall onto a waste package surface are likely to drain down the surface before entering a patch opening. Therefore, the flux of water (i.e., rivulets flowing down the surface of the waste package) intercepted by patches, and thereby entering a waste package, is determined by considering the uncertainty in the rivulet spread angle and ignoring interference by multiple patches (SNL 2007, Section 6.3.3.2.5). This model predicts more flow than a flow model that is proportional to the total area of waste package patches. As described in SAR Section 2.4.2.3.2.1.6, the flow splitting fraction reaches a value of 1 (i.e., all the impinging flow can enter a waste package) well before the number of patches reaches its maximum. For the mean value of 1.2 for the waste package flux-splitting uncertainty distribution, only about 62 general corrosion patches (out of a total of 1,430) are required on a commercial spent nuclear fuel waste package to allow 100% of the impinging flow to enter a waste package (SNL 2008, Section 6.3.6.2). This is only 4% of the area of the waste package (excluding the lids). The flux splitting model used in the nominal scenario to determine the amount of seepage flowing down the sides of a breached waste package that may intersect a patch opening is not applicable in the human intrusion scenario, where the location of the borehole breach in the intruded waste package always occurs along the waste package crown (SNL 2008, Section 6.7.2.3.3).

In the human intrusion scenario, where the drill patch opening occurs along the crown of the waste package, the fraction of dripping flux falling on the crown of the waste package that flows into the waste package is expected to be proportional to the area of patch opening. Using the post-10,000-year repository average seepage from the nominal modeling case, 9.47×10^{-2} m^3/yr without the flux splitting model, the calculated seepage flux through a single patch in the nominal scenario class is lower, varying between 7.27×10^{-6} and 2.67×10^{-4} m^3/yr, based on the 5th and 95th percentile values of the seepage flux distribution, and having a mean value of 7.82×10^{-5} m^3/yr. Likewise, the calculated seepage flux through 1.4 patches is reduced to a range between 1.02×10^{-5} and 3.74×10^{-4} m^3/yr, based on the 5th and 95th percentile values of the seepage flux distribution, with a mean of 1.09×10^{-4} m^3/yr.

Table 2. Comparison of Water Flux through a Borehole Opening and a Nominal Patch – Post-10,000 Years

Post-10,000-Year Repository Average Flow Rates (m^3/yr/waste package)			
	5th percentile	**Mean**	**95th percentile**
Human Intrusion Modeling Case			
Mean flow through human intrusion borehole	4.78×10^{-4}	1.03×10^{-3}	2.28×10^{-3}
Nominal Modeling Case - Mean Seepage			
Flow through single nominal patch	1.42×10^{-4}	1.53×10^{-3}	5.22×10^{-3}
Flow through 1.4 nominal patches	1.99×10^{-4}	2.13×10^{-3}	7.30×10^{-3}
Nominal Modeling Case - Mean Seepage (without flux splitting model)			
Flow through single nominal patch	7.27×10^{-6}	7.82×10^{-5}	2.67×10^{-4}
Flow through 1.4 nominal patches	1.02×10^{-5}	1.09×10^{-4}	3.74×10^{-4}

Source: Percolation flux from Table 3 of response to RAI 3.2.2.1.3.6-005; nominal seepage from Table 5 of response to RAI 3.2.2.1.3.6-2-010; and spreadsheet: *HIFluxvsFulxSplit_v1.xls*.

1.3 SUMMARY

The use of the percolation flux at the base of the PTn unit to determine the volumetric flow rate of water through the intruded waste package is considered to be representative of steady-state conditions consistent with the conceptualization of the degraded borehole.

An estimation of the mean water flux from impinging seepage that may enter the breached area of the waste package caused by the intrusion is approximately 3.5%. A comparison of the mean water flux through a borehole patch in the human intrusion scenario to the water flux through a single patch failure in the nominal scenario shows that the mean flow through the borehole opening in the intruded waste package is lower than the mean seepage that could flow through a single patch in the nominal modeling case which includes the effects of flux splitting model. Without the flux splitting model, the mean flow through a single patch in the nominal modeling case is much lower than the mean flow through the borehole opening in the intruded waste package. The occurrence of any additional water flux through the intruded waste package as a result of impinging seepage near the borehole breach is captured in the analyses and will not impact the peak mean annual dose projections for the human intrusion scenario.

2. COMMITMENTS TO NRC

None.

3. DESCRIPTION OF PROPOSED LA CHANGE

None.

4. REFERENCES

BSC (Bechtel SAIC Company) 2003. *Atlas Breached Waste Package and Drip Shield Experiments: Breached Drip Shield Tests*. TDR-EBS-MD-000025 REV00. Las Vegas, Nevada: Bechtel SAIC Company. ACC: DOC.20030619.0001.

SNL (Sandia National Laboratories) 2007. *EBS Radionuclide Transport Abstraction*. ANL-WIS-PA-000001 REV 03. Las Vegas, Nevada: Sandia National Laboratories. ACC: DOC.20071004.0001.

SNL 2008. *Total System Performance Assessment Model/Analysis for the License Application*. MDL-WIS-PA-000005 REV 00 AD 01. Las Vegas, Nevada: Sandia National Laboratories. ACC: DOC.20080312.0001.

RAI Volume 3, Chapter 2.2.1.4.2, First Set, Number 2:

> Clarify the technical basis for delay of radionuclide transport due to matrix diffusion in the borehole.
>
> Basis: Advective flow of water in the borehole potentially results in very short travel times (e.g., on the order of a few years) in the borehole when fracture-matrix interactions are ignored (see section 2.4.3.3.5.1 of the SAR, page 2.4-316). The SAR suggests that sorbing radionuclides are delayed significantly due to matrix diffusion (Figure 2.4-170). But the supporting information does not clearly explain the basis for how the relatively slow matrix diffusion process has such a significant effect given the very short travel times and the limited time over which the matrix diffusion process can occur. The staff needs this information to determine compliance with 10 CFR Part 63.114.

1. RESPONSE

An assessment of an inadvertent human intrusion is performed with the total system performance assessment (TSPA) model to demonstrate compliance with the individual protection standard for human intrusion (10 CFR 63.321). The assumptions set forth in 10 CFR 63.322 are used to develop the stylized analysis, which incorporates other aspects of the TSPA model that account for uncertainties and variability in the geology, hydrology, and geochemistry of the Yucca Mountain site and the surrounding vicinity, and also account for the degradation, deterioration, or alteration processes of the Engineered Barrier System (EBS), as set forth in 10 CFR 63.114.

The human intrusion modeling case transports radionuclides released from a single intruded waste package vertically downward through the borehole. The borehole extends 190 m from the bottom of the waste package, through the unsaturated zone, to the saturated zone. The borehole is conceptualized to be an uncased, degraded borehole that has matrix and fracture properties of the unsaturated zone rock types comprising the repository horizon. The rubble fill in the borehole is considered to have properties similar to the undisturbed repository host rock matrix, while any preferential pathways within the rubble fill are given fracture properties of the host rock. As a result, the collapsed matrix blocks are expected to occupy about 99% of the borehole volume, while about 1% of the borehole volume is occupied by the fracture (consistent with the fracture porosity of the undisturbed rock) (SNL 2008, Section 6.7.3.2). The fracture and matrix volumes represent a simplified estimate of the effective porosity in the borehole fracture. The low effective porosity in the fracture results in faster flow velocities through the fracture. A dual-porosity approach is adopted by modeling a discrete fracture that is surrounded by the rock matrix. Transport through the borehole is modeled using the GoldSim pipe pathway element configured as two parallel plates fully surrounded by a porous medium. Fracture flow occurs vertically between the walls of the fracture. The rate of water flow in the borehole is the product of the percolation flux (mm/yr) at the base of the Paintbrush Tuff nonwelded (PTn) unit and the borehole cross-sectional area. However, communication with the matrix in the degraded borehole retards the rate of transport of radionuclides from the repository horizon to the saturated zone.

1.1 MATRIX DIFFUSION

Matrix diffusion is a transport mechanism by which solutes, the released inventory from the intruded waste package, are transferred between the water-flowing portions of the fracture to the non-flowing portions of the matrix. The transport equation for a solute in the borehole fracture with matrix diffusion, Equation 1, is the advection-dispersion equation with an additional storage term for the transport across the fracture–matrix boundary.

$$\frac{\partial c}{\partial t}+\frac{v}{R}\frac{\partial c}{\partial z}-\frac{\alpha_L v+D^*}{R}\frac{\partial^2 c}{\partial z^2}-\frac{\theta\tau D^*}{sbR}\frac{\partial c'}{\partial x}\bigg|_{x=b}=0 \qquad \text{(Eq. 1)}$$

where

c = the concentration of the radionuclide in fracture

t = time

v = groundwater velocity in the fracture

R = retardation coefficient in the fracture

α_L = longitudinal dispersivity

D^* = molecular diffusion coefficient in free solution

θ = water content of the matrix (product of the matrix porosity and matrix saturation)

s = fracture saturation

τ = matrix tortuosity

b = distance from the fracture center to the fracture edge (the half-width of the fracture)

c' = concentration of the radionuclide in the matrix

z denotes the vertical direction along the fracture

x denotes the horizontal direction in the matrix.

The concentration of the radionuclide in the matrix is defined by Equation 2.

$$\frac{\partial c'}{\partial t}-\frac{\tau D^*}{\left(1+\frac{\rho_b}{\theta}K_m\right)}\frac{\partial^2 c'}{\partial x^2}=0 \qquad \text{(Eq. 2)}$$

where

ρ_b = the bulk density of the matrix

K_m = the distribution coefficient for the matrix.

Equations 1 and 2 provide the transport equations for a non-decaying solute. For decay chains, additional terms are included to account for both decay and decay product growth.

The TSPA model utilizes the pipe pathway element of the GoldSim Radionuclide Transport module to provide the solution. The pipe pathway model includes the additional terms for radionuclide decay and decay product growth.

1.2 GOLDSIM PIPE PATHWAY CONFIGURATION

In the TSPA model, radionuclide transport through the borehole is modeled using the GoldSim pipe pathway element. The conceptual model of the borehole is depicted in Figure 6.7-6 of *Total System Performance Assessment Model/Analysis for the License Application* (SNL 2008), which is reproduced as Figure 1. Vertical transport down the unsaturated fracture is represented as two parallel plates with no infill between the plates. The distance between the plates is the average fracture aperture for the rock units comprising the devitrified tuff of the repository horizon, which includes the host-rock units TSw34, TSw35, and TSw36, with the width of the plates determined by the size of the borehole. Molecular diffusion occurs between the fracture and borehole rubble surrounding the fracture, and then through the porous medium. Radionuclide decay and decay product growth occur in both the fracture and the matrix. Although no sorption is modeled in the fractures for any radionuclide, sorption is modeled in the matrix. Consistent with the treatment in the three-dimensional unsaturated zone transport model, the partition coefficients for sorption in the matrix are those for devitrified tuff. The input parameters for the borehole transport model are defined in Table 1.

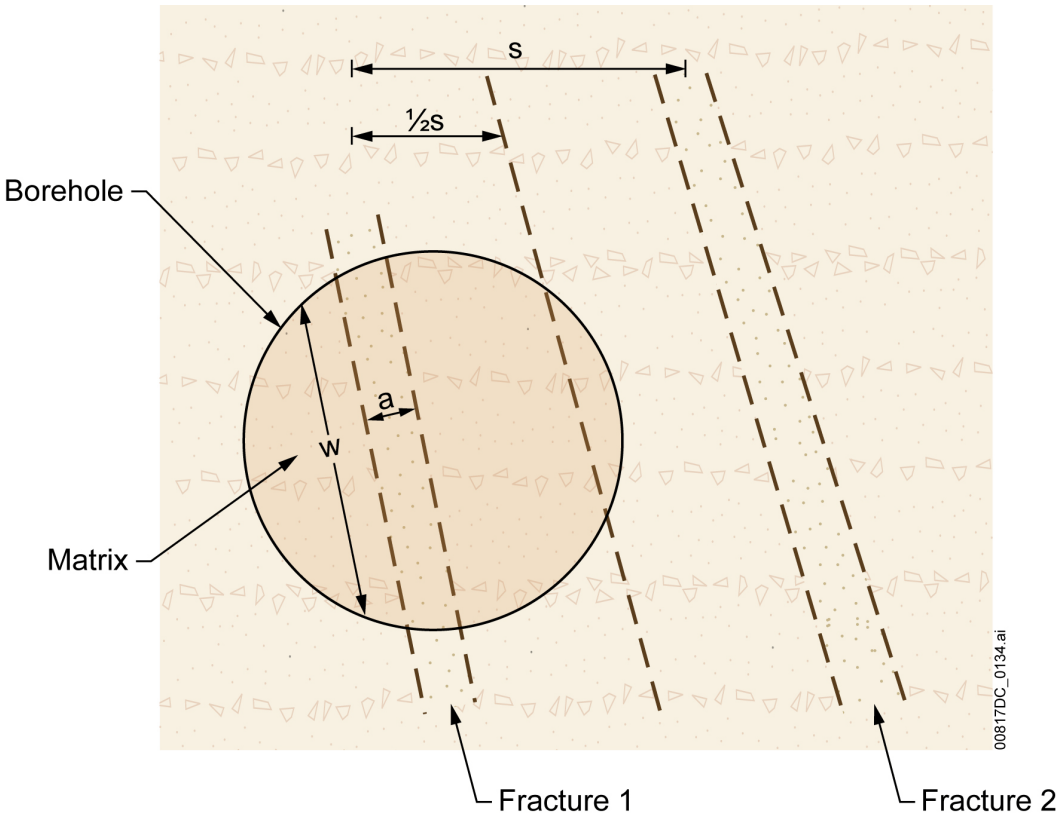

w = fracture width
s = fracture spacing
a = fracture aperture
½s = diffusion length between fracture and matrix
Borehole = Drill Patch Area = 0.0324 m^2

Figure 1. Schematic Depiction of Borehole (map view) with a Bisecting Fracture

Table 1. Matrix Diffusion Pipe Pathway Parameter Values

Parameter	Value	Description
Borehole diameter[a]	8 inches	Input: The diameter of the human intrusion borehole
Borehole length[a]	190 m	Input: The length of the human intrusion borehole
Fracture aperture[a]	0.00264 m	Input: Distance between fracture openings in unsaturated zone borehole
Fracture width[a]	~0.160 m	Calculated: Width of the unsaturated zone borehole fracture
Fracture area[a]	~0.000421 m^2	Calculated: Cross-sectional area of the unsaturated zone borehole fracture
Fracture perimeter[a]	~0.324 m	Calculated: The perimeter of the unsaturated zone borehole fracture
Borehole dispersivity[a]	10 m	Input: The dispersivity in the unsaturated zone borehole fracture
Fracture saturation[b]	Varies by percolation subregion and infiltration case	Input: The average saturation in the unsaturated zone borehole fracture
Matrix thickness[a]	~0.125 m	Calculated: Thickness of the matrix zone surrounding the unsaturated zone borehole
Matrix saturation[b]	Varies by percolation subregion and infiltration case	Input: The average saturation in the unsaturated zone matrix surrounding the unsaturated zone borehole fracture
Matrix porosity[c]	0.149	Calculated: Average matrix porosity for the unsaturated zone rock group that contains the devitrified tuff units of the repository horizon
Matrix density[c]	1,980 kg/m^3	Bulk dry density of matrix rock, tsw35
Matrix tortuosity (mean) (log value)[d]	−1.84	The mean value of a normal distribution for the tortuosity of the matrix (Dm/D*) for the unsaturated zone rock group that contains the devitrified tuff units of the repository horizon
Matrix tortuosity (standard deviation) (log value)[d]	0.29	The standard deviation of a normal distribution for the tortuosity of the matrix (D_m/D*) for the unsaturated zone rock group that contains the devitrified tuff units of the repository horizon
Reference diffusivity	2.80×10^{-10} m^2/s	Calculated: Mean molecular diffusion coefficient in free solution for non-colloidal species

Sources: [a]SNL 2008, Section 6.7.3.2, Tables 6.7-5 and Table 6.7-6.
[b]SNL 2008, Tables 6.3.8-4 and 6.3.8-5.
[c]SNL 2007, Table 8.2-6
[d]SNL 2008, Table 6.3.9-4.

The conceptualized human intrusion borehole is an 8-inch diameter borehole that extends 190 m from the bottom of the waste package to the highest expected water table elevation. The borehole is modeled with a rectangular fracture area equal to the product of the unsaturated zone fracture aperture and the average width of the unsaturated zone fracture. The average width of the fracture is calculated by dividing the borehole cross-sectional area by its diameter. The fracture pathway has an average saturation of 0.0234, but the saturation varies by percolation subregion and infiltration case. This average value is the weighted average of the fracture saturation applied in the unsaturated zone transport model. Saturation values for each infiltration case and percolation subregion are weighted by a factor that accounts for the probability of each infiltration case and the probability of the human intrusion intersecting each percolation subregion. The reference fluid in the fracture pathway is water and imposes no solubility limits.

The pipe pathway is configured with no coating, no suspended solids, and no stagnant zone. The pipe pathway has one matrix diffusion zone. Bidirectional diffusion between the fracture and the matrix is one-dimensional and is orthogonal to the flow direction. The matrix diffusion zone is configured with no skin, is filled with unsaturated zone matrix medium, and has a constant thickness that is one-half of the applied distance between fractures in the unsaturated zone around the entire perimeter of the aperture. The outside edge of the matrix has a zero gradient boundary condition. At the inside edge of the matrix, the aqueous concentration in the matrix is equated to the aqueous concentration in the fracture. The matrix zone is modeled with a slab geometry and the diffusive area remains constant through the thickness of the matrix. Multiplying the fracture perimeter by the matrix thickness yields an effective area, the area in a cross-section perpendicular to the flow direction, of 0.0408 m^2. The average saturation of the matrix is 0.980, but the saturation varies by percolation subregion and infiltration case. This average value is the weighted average of the matrix saturation applied in the unsaturated zone transport model. Saturation values for each infiltration case and percolation subregion are weighted by a factor that accounts for the probability of each infiltration case and the probability of the human intrusion intersecting each percolation subregion. The tortuosity of the unsaturated zone matrix is the applied value for the tortuosity of the unsaturated zone rock group that contains the devitrified tuff units of the repository horizon, which varies log-normally and has a median value of 0.0145 and a mean value of 0.0181. The reference fluid in the matrix diffusion zone is water and imposes no solubility limits. The diffusivity for non-colloidal radionuclides in the free solution is the same as that imposed in the Engineered Barrier System. Using the mean value for the diameter of a colloid and the relative diffusivity for a noncolloidal species (=100), the mean value for the reference diffusivity is 2.80×10^{-10} m^2/s.

GoldSim solves the coupled set of transport and decay equations in the pipe pathway using Laplace transforms. The GoldSim solution was compared to theoretical expectations and other software codes for verification.

1.3 SIGNIFICANCE OF MATRIX DIFFUSION

In the absence of matrix diffusion, the average volume of water in the fracture (190-m borehole length applied across the fracture cross-sectional area (0.000421 m^2) in the saturated part of the fracture (0.0234)) is 0.00187 m^3 and has a residence time of 1.81 years when the average percolation flux for the post-10,000-year climate (31.83 mm/yr) is applied across the original 8-inch-diameter borehole. This estimate is consistent with the value reported in SAR Section 2.4.3.3.5.1, which estimates an approximate 3-year travel time applying a 26.9 mm/yr percolation rate and a fracture saturation of 0.025. However, the inclusion of matrix diffusion greatly retards transport through the borehole for both sorbing and non-sorbing contaminants. The significance of the matrix diffusion process can be conceptualized by examining Equations 1 and 2.

The second and third terms in Equation 1, $\frac{v}{R}\frac{\partial c}{\partial z}$ and $-\frac{\alpha_L v + D^*}{R}\frac{\partial^2 c}{\partial z^2}$, respectively, represent advection and dispersion in the vertical direction of the borehole. The fourth term, $-\frac{\theta\tau D^*}{sbR}\frac{\partial c'}{\partial x}\Big|_{x=b}$, is the effect of matrix diffusion across the fracture–matrix boundary. For matrix diffusion to have a significant effect on transport in the borehole, the relative contribution of the fourth term in Equation 1 must be greater than the sum of the contributions from the second and third terms. Parameter values that increase the relative contributions of the second and third terms or reduce the contributions of the fourth term decrease the effectiveness of matrix diffusion. Therefore, increasing the groundwater velocity down the borehole decreases the effectiveness of matrix diffusion to retard solutes in the pipe pathway. Increasing the porosity of the matrix, the tortuosity of the matrix, or the diffusivity of the solute in the matrix, or decreasing the fracture aperture, increases diffusion from the fractures in the matrix. Furthermore, parameters that increase the concentration gradient along the length of the matrix, as described by Equation 2, also increase the effectiveness of matrix diffusion.

Significant parameters affecting concentration gradients in the matrix are saturation, porosity, tortuosity, diffusivity, and partition coefficients. Increases in the porosity and saturation of the matrix increase the water volume in the matrix. Greater water volumes can result in lower matrix concentrations, which will increase the diffusive gradient into the matrix. Similarly, increasing the diffusivity in the matrix, by changing the tortuosity of the matrix, increases the movement of radionuclides in the matrix, which allows radionuclides to move into the matrix further and faster until concentrations in the matrix attain equilibrium. Increasing partition coefficients increases the amount of solute that sorbs to the solid phase, reducing aqueous concentrations in the matrix and increasing the diffusive gradient into the matrix. The higher the partition coefficient, the greater the effect of matrix diffusion. The thickness of the matrix, the length of the *x* direction in Equation 2, also affects the contribution of matrix diffusion; the thicker the matrix, the longer the distance from the zero gradient boundary, and the greater the concentration gradient through the matrix is extended. In addition, a thicker matrix has a greater volume of the porous medium, which increases the capacity of the matrix for sorption.

Within the TSPA model, the selection of borehole parameter values balances the relatively high linear flow rate through the borehole with the matrix diffusion process. A non-sorbing species, such as ^{129}I, is still retarded when matrix diffusion is considered, increasing the travel time from three years to approximately 1,250 years (SNL 2008, Section 7.2.4.1.12[a], Figure 7.2-17[a]). Without sorption in the matrix, this delay is attributed to the lateral movement of ^{129}I into the matrix by diffusion. For a non-sorbing radionuclide, the contribution of matrix diffusion is determined by the tortuosity in the matrix and free water diffusivity, which govern the lateral movement of mass into the matrix in accordance with a concentration gradient that initially has no matrix mass. Transport delay times increase for radionuclides with partition coefficients.

1.4 VERIFICATION ACTIVITIES

The TSPA model uses the GoldSim pipe pathway element to solve the transport equations for mass introduced into the borehole.

The verification of the borehole transport model is described in Section 7.2.4.1.12[a] of *Total System Performance Assessment Model/Analysis for the License Application* (SNL 2008). The verification activity transports 1 gram each of ^{129}I and ^{237}Np through a borehole with and without matrix diffusion. With the exception of the borehole flux, which was specified to be 25 mm/yr, the sampled uncertainties that affect transport in the unsaturated zone borehole (e.g., fracture saturation, matrix saturation, matrix partition coefficients, and matrix tortuosity) in the verification case match the values applied in at least one realization of the human intrusion model case. When matrix diffusion is disabled, 99.98% of the ^{129}I and ^{237}Np mass that enters the borehole is released from the borehole in the first 250-year time step. Some of the mass of ^{237}Np is converted to its decay products, ^{233}U and ^{229}Th. When matrix diffusion is enabled, the time required for 50% of the released mass to exit the bottom of the borehole increases by approximately 1,250 years for the nonsorbing radionuclide ^{129}I and by approximately 64,000 years for the moderately sorbing radionuclide ^{237}Np. The ratio of the delay times, 51.2, is approximately equal to the ratio of the matrix retardation factors, 47.8, which is determined by the difference in partition coefficients for the two radionuclides.

To verify that the results of the borehole transport model in the human intrusion modeling case do not show an excess influence of matrix diffusion, the results of a GoldSim pipe model were compared to the results using an analytical solution presented by Sudicky and Frind (1982). This analytical solution describes the transport of dissolved species in parallel fractures subject to matrix diffusion. With one exception, the GoldSim pipe model in this verification analysis is configured similarly to the borehole transport model found in single realization analysis of the human intrusion modeling case (SNL 2008, Section 7.7.1.6[a]). The exception is that a constant mass flux into the fractures at the upgradient boundary of the borehole is applied. This constant flux boundary condition is used to allow for a comparison to the analytical solution and is similar to the flux boundary condition in the single realization analysis. Note that the analytical solution presented by Sudicky and Frind (1982) is derived to solve for concentrations in the fractures at a point of interest, and is based on a constant concentration upgradient boundary condition.

A general solution for the Laplace transformed governing equation of solute transport through a parallel set of fractures subject to matrix diffusion is presented by Sudicky and Frind (1982). The analytical solution used to verify the GoldSim pipe pathway model is based on this formulation and is solved by numerically inverting the solution from the Laplace domain using the DeHoog algorithm presented by Moridis (1998).

Two sets of simulations comprising a stand-alone GoldSim pipe model simulation and an alternative analytical solution simulation were performed to verify that the results of the TSPA human intrusion pipe model are as expected and do not show an excess influence of matrix diffusion. The first set of simulations assumed that the dissolved species was technetium, a conservative species that does not sorb onto the rock matrix. The second set of simulations assumed that the dissolved species was plutonium, a highly sorbing species with a matrix

retardation of 1,550 (SNL 2008, Section 7.7.1.6[a]). The parameters used in the analysis that differ from those presented in Table 1 are listed in Table 2 and are taken from Realization 8309 of the human intrusion modeling case described in *Total System Performance Assessment Model/Analysis for the License Application* (SNL 2008, Section 7.7.1.6[a]).

Table 2. Matrix Diffusion Pipe Pathway Parameter Values: Verification Analysis

Parameter	Value	Description
HI_Borehole_Seepage	0.0008728 m^3/yr	Volumetric flow rate through fractures based on repository percolation rate for the post-10,000 year climate
UZ_Matrix_Tortuosity	0.0129	Tortuosity (D_m/D^*) for rock group 3
Ref_Diffusivity	1.79×10^{-10} m^2/sec	Molecular diffusion coefficient in free solution for non-colloidal species
f_perimeter_md	1.0	The fraction of the fracture perimeter that is in contact with the matrix
HI_UZ_Fracture_Saturation	0.0253	Saturation in the unsaturated zone fractures
HI_UZ_Matrix_Saturation	0.987	Saturation in the unsaturated zone matrix
Fracture Width	0.1595 m	The width of the fracture in the pipe
Retardation (Technetium)	1.0	The retardation for iodine
Retardation (Plutonium)	1,550	The retardation for plutonium

The source term for the two simulations is a constant mass flux of 1 g/yr and the results are presented in normalized mass fluxes through the fractures at 190 m from the source. In addition, radionuclide decay is not considered in the simulations in order to simplify the analysis of the two major processes, advective-dispersive transport and matrix diffusion. There are minor differences in the geometry of the GoldSim and analytical solutions. In the analytical solution, the direction of the fractures in a planar view is infinite; in the GoldSim solution, the pipe is finite. Therefore, the effective diffusive area for the pipe, where diffusion can take place at the end of the fracture, is approximately 1.02 (0.324 m/(2 × 0.1595 m)) times greater than for the analytical solution.

Figure 2 presents a comparison of the results of the GoldSim pipe model and the analytical solution based on the Sudicky and Frind (1982) solution for transport of technetium through the fractures. The close agreement between the mass flux results for the two solution techniques, despite the 2% difference in the effective diffusive area at the end of the fracture, verifies that the GoldSim solution does not show an excess influence of matrix diffusion for a non-sorbing species.

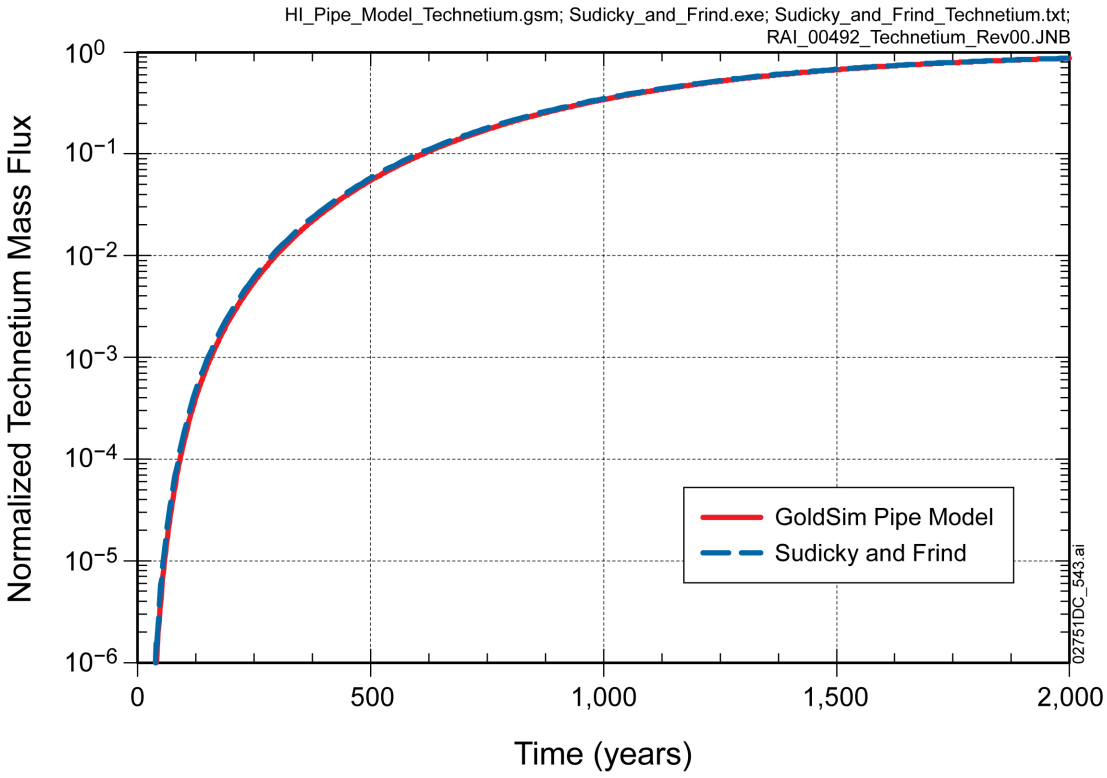

Figure 2. Comparison of Normalized Technetium Mass Flux Releases Generated Using a Stand-Alone Version of the Human Intrusion Pipe Model and an Analytical Solution by Sudicky and Frind (1982)

Note that despite the fact that the average linear velocity through the fracture is approximately 82 m/yr in this analysis, it takes approximately 1,250 years for the median breakthrough (the breakthrough when the mass flux at 190 m reaches one-half of the boundary flux or a normalized flux of 0.5) to occur. These results show that the relatively slow matrix diffusion process can have a significant effect despite the very short advection-based travel times and the limited time over which the matrix diffusion process can occur. This long time period is indicative of the effectiveness of matrix diffusion in retarding the transport of radionuclides for the fracture geometry (fracture water volume versus diffusive surface area) defined for this simulation.

Figure 3 presents a comparison of the results of the GoldSim pipe model and the analytical solution based on Sudicky and Frind (1982) for transport of plutonium through the fractures. Again, the close agreement between the mass flux results for the two solution techniques verifies that the GoldSim solution does not show an excess influence of matrix diffusion for a highly sorbing species.

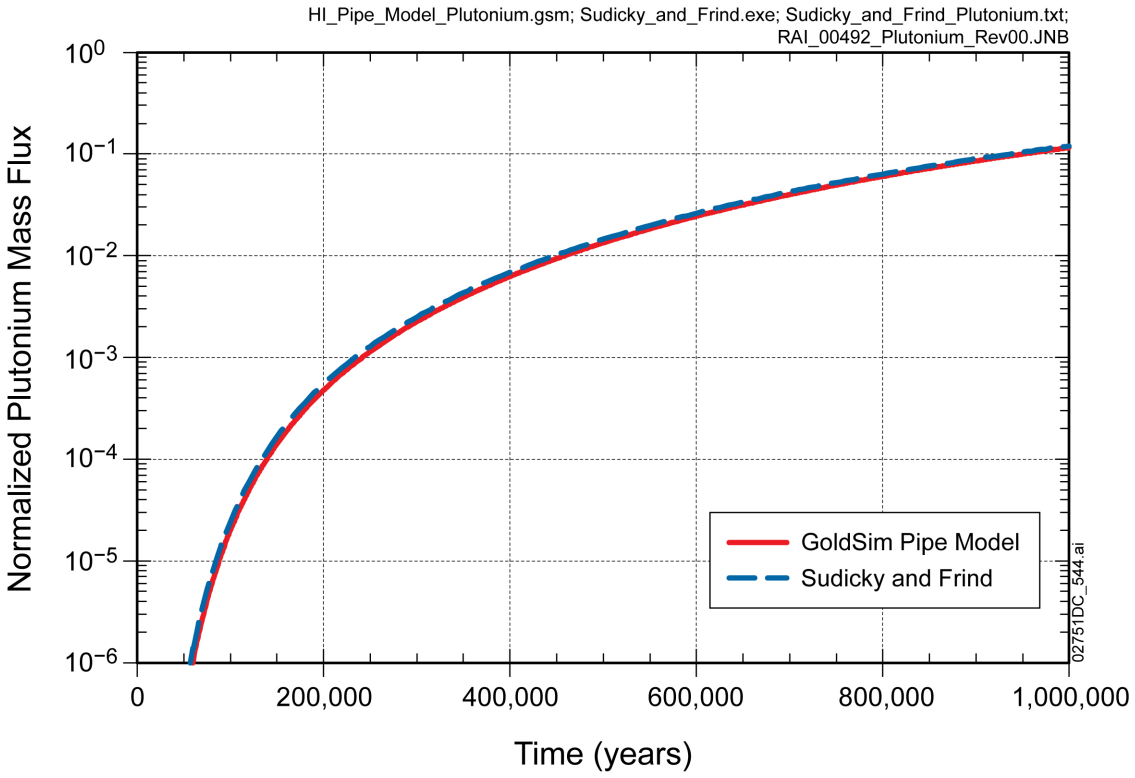

Figure 3. Comparison of Normalized Plutonium Mass Flux Releases Generated Using a Stand-Alone Version of the Human Intrusion Pipe Model and an Analytical Solution by Sudicky and Frind (1982)

For the highly sorbing species, plutonium, it takes over 1,000,000 years for 50% of the initial mass to be released from the bottom of the borehole. These results again show that the relatively slow matrix diffusion process can have a significant effect despite the very short advection-based travel times. The extremely long travel time associated with a highly sorbing species, compared to the non-sorbing species, reflects the large storage capacity in the rock matrix, associated with the sorption that promotes the continuity of a large diffusive gradient into the matrix for an extremely long period of time and delays the occurrence of concentration equilibrium between the fractures and rock matrix.

1.5 CONFIGURATION PARAMETER SENSITIVITY

The verification activities described in the previous section demonstrate that the solution applied in GoldSim is accurate for the problem as it is configured. Using the pipe solution in GoldSim, the properties of the pipe pathway that contribute significantly to the delay are examined. In these sensitivity runs, a GoldSim model is built that matches the configuration in the TSPA model human intrusion modeling case, with the exception that 1 kg of a low sorbing, non-decaying species is applied as an instantaneous input into the pipe pathway. The properties of selected parameters are then modified and the time required to discharge 50% of the initial mass is compared. Table 3 provides the base-case configuration parameters for the pipe model that differ from those presented in Table 1. Table 4 provides the range of test conditions used to

evaluate the sensitivity of the transport model to the transport parameters. Reductions and increases in the parameter values up to factors of 1,000 may generate physically unrealistic scenarios. For instance, increasing the matrix porosity to 0.745, a value that is five times the base-case value, is not a realistic value for matrix media. Therefore, some of the results of this sensitivity are simply numerical solutions that do not represent a realistic physical system. In the sensitivity test cases, only one parameter is varied at a time. Figure 4 plots the time of 50% breakthrough for the different test cases.

Table 3. Matrix Diffusion Pipe Pathway Sensitivity: Base-Case Parameter Values

Parameter	Value	Description
UZ_Matrix_Tortuosity	0.0145	Mean value for the tortuosity (D_m/D^*) for rock group 3
Ref_Diffusivity	1.73×10^{-10} m^2/s	Molecular diffusion coefficient in free solution for non-colloidal species
Percolation_Rate	31.83 mm/yr	Mean repository percolation rate for the post-10,000-year climate
HI_Borehole_Seepage	0.00103 m^3/yr	Volumetric flow rate down an 8-inch borehole at the applied percolation rate of 31.83 mm/yr
UZ_Matrix_Kd	1 ml/g	Partition coefficient in the matrix
HI_UZ_Fracture_Saturation	0.0234	Weighted average saturation in the unsaturated zone fractures
HI_UZ_Matrix_Saturation	0.98	Weighted average saturation in the unsaturated zone matrix

Table 4. Matrix Diffusion Pipe Pathway Sensitivity: Sensitivity Case Parameter Values

Case	Parameter	Value
1	Percolation_Rate	Method 2
2	UZ_Matrix_Kd	Method 2
3	f_perimeter_md	Method 3
4	Matrix Thickness	Method 1
5	UZ_Matrix_Tortuosity	Method 2
6	Ref_Diffusivity	Method 2
7	UZ_Matrix_Porosity	Method 1
8	HI_UZ_Fracture_Saturation	Method 3
9	HI_UZ_Matrix_Saturation	Method 3
10	HI_UZ_Borehole_Disp	Method 1

NOTES: Method 1: Values are 0, 10%, 25%, 50%, 75%, 90%, 100%, 200%, 300%, 400%, and 500% of the base-case values.

Method 2: Values are 0.1%, 1%, 10%, 25%, 50%, 1×, 2×, 4×, 10×, 100×, and 1,000× the base-case values.

Method 3: Values are 0 (or 0.01), 0.1, 0.2, 0.3, 0.4, 0.5, 0.6, 0.7, 0.8, 0.9, and 1.0.

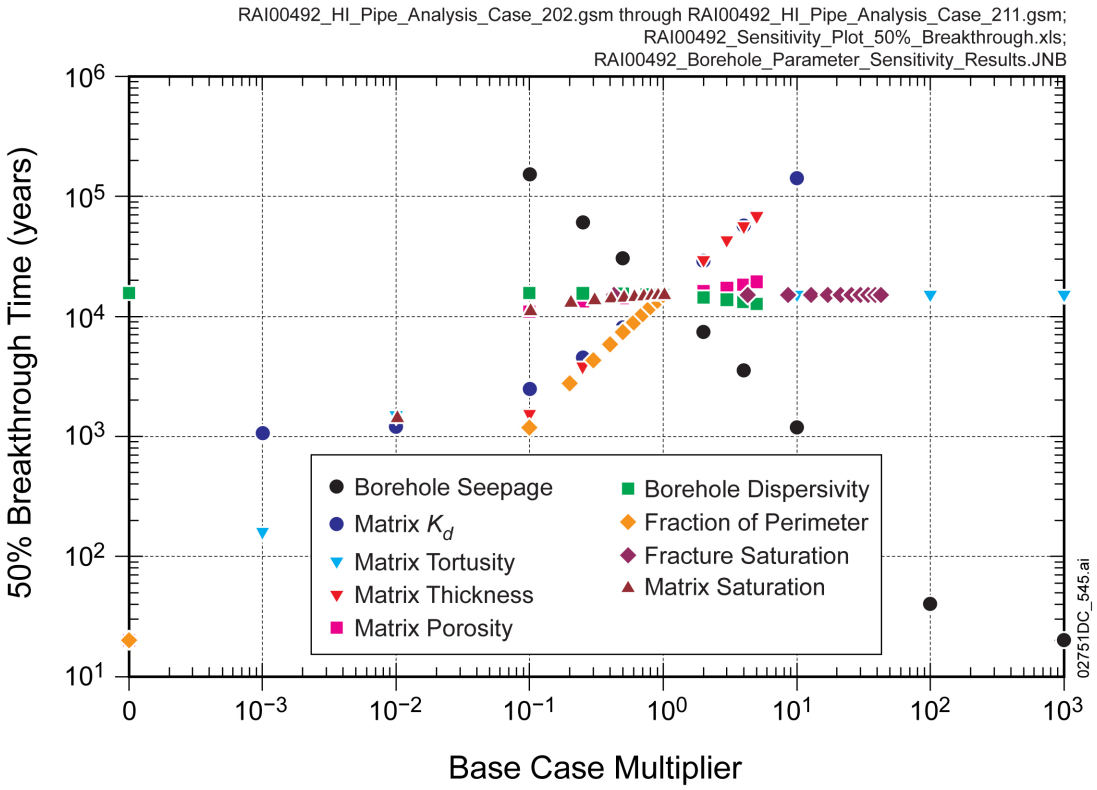

Figure 4. Human Intrusion Pipe Pathway Sensitivity Results on 50% Breakthrough Time for an Instantaneous Input

1.5.1 Sensitivity to Percolation Rate

In this sensitivity analysis, the base-case model percolation rate is reduced and increased by factors up to 1,000. When matrix diffusion is considered, the flow rate down the borehole has a significant effect on the release of the solute from the borehole. Increases in the percolation rate increase the sum of the contribution of the second and third terms in Equation 1. For a flux rate that is 1/100th of the repository-wide average or slower, breakthrough to the 50% level is not attained within 1,000,000 years. Above 10% of the repository-wide percolation flux, the breakthrough time decreases exponentially for increases in the flux rate.

1.5.2 Sensitivity to Partition Coefficient

In this sensitivity analysis, the base-case model partition coefficient is reduced and increased by factors up to 1,000. When matrix diffusion is considered, the partition coefficient for sorption in the matrix also has a significant effect on transport through the borehole. Increases in the partition coefficient directly affect Equation 2, which is coupled with the fourth term in Equation 1. When very little sorption to the matrix is modeled, K_d = 0.001 ml/g, the time required to achieve 50% breakthrough is about 1,060 years at the repository-wide average percolation rate. By comparison, a K_d of 100 ml/g, a value comparable to the K_d of plutonium in

devitrified tuff, does not attain 50% breakthrough in 1,000,000 years. For a K_d value of 0.5 ml/g, the median value for ^{237}Np, it takes approximately 8,040 years to attain 50% breakthrough.

Sorption in the matrix has a retardation and a diffusion effect. In addition to rendering sorbed mass immobile, albeit temporarily, sorption reduces the aqueous concentration in the matrix, which subsequently increases the diffusion gradient across the fracture–matrix interface, resulting in an increased effect of matrix diffusion.

1.5.3 Sensitivity to Matrix–Fracture Interface Area

In this sensitivity analysis, the base-case model fraction of the fracture perimeter that is surrounded by rubble is changed from 0% to 100% of the base-case value. This has the effect of reducing the effective area for transport between the fracture–matrix interface. Decreasing the interface area reduces diffusion out of the fractures. Using a zero diffusive area is comparable to eliminating matrix diffusion. Cutting the diffusive area to 10% of the perimeter reduces the 50% breakthrough time from approximately 15,000 years to approximately 1,180 years. A reduction of 50% in diffusive area reduces the 50% breakthrough time to 7,380 years. Decreasing the diffusion area reduces diffusion across the fracture–matrix interface but also reduces the storage capacity of the matrix by reducing the volume of matrix available for sorption.

1.5.4 Sensitivity to Matrix Thickness

In this sensitivity analysis, the base-case model thickness of the matrix surrounding the fracture is changed from 0% to 500% of the base-case value. The thickness of the matrix defines the diffusive length from the fracture to the zero gradient boundary at the outside edge of the matrix. Increasing and decreasing the thickness of the matrix also has the effect of reducing and increasing the volume of the matrix available for diffusion and sorption. Reducing the matrix to 0 m is equivalent to excluding matrix diffusion. With no matrix thickness, the time to attain 50% breakthrough is lower than the applied 20-year time step length. Reducing the matrix thickness to 10% of the base-case value reduces the 50% breakthrough time from 15,000 to 1,540 years. Doubling the matrix thickness nearly doubles the 50% breakthrough time, which occurs at approximately 29,500 years. However, the cumulative mass released from the pipe pathway does not change for greater matrix thicknesses until well into the simulation time. For the two longest thicknesses, the cumulative release is the same until around 10,000 years. This result demonstrates that increasing the diffusion distance into the matrix only affects releases once sufficient time has elapsed to permit the solute to diffuse across the entire thickness of the matrix.

1.5.5 Sensitivity to Matrix Tortuosity and Diffusivity

In this sensitivity analysis, the base-case matrix tortuosity is reduced and increased by factors up to 1,000. Because this term is coupled with the effective diffusivity in Equations 1 and 2, this change reflects changes in the free water diffusivity. Changes in the tortuosity/diffusivity have a mixed effect on the 50% breakthrough time. For the smallest value of the parameter, 1/1000th of the base-case value, the breakthrough time decreases to 160 years. The low tortuosity and low diffusivity hamper diffusion out of the fractures and into the matrix. Values above this low value

of tortuosity/diffusivity increase the time required to attain 50% breakthrough, but the increased time is not proportional to the increase in the parameter. As tortuosity/diffusivity increases, the effect of matrix diffusion to retard transport increases by allowing mass to exit the fractures. However, the increase in the tortuosity/diffusivity has diminishing returns as the breakthrough times for tortuosity values from 25% up to 1,000 times the base-case value are nearly identical. The higher the tortuosity/diffusivity, the easier mass can diffuse from the fractures; however, increased tortuosity/diffusivity also allows mass to equilibrate in the matrix faster and diffuse back into the fractures faster as the source term approaches depletion and the concentration gradient changes direction.

1.5.6 Sensitivity to Matrix Porosity

In this sensitivity analysis, the base-case matrix porosity is changed from 0% to 500% of the base-case value. This has the effect of reducing and increasing the volume of matrix water available for transport in the matrix. Decreasing the matrix porosity to 0 is equivalent to excluding matrix diffusion, as Equation 1 reduces to the simple advection dispersion equation without matrix diffusion. With no matrix porosity, the time to attain 50% breakthrough is lower than the applied 20-year time step length. Because of its presence in Equations 1 and 2, other changes in the matrix porosity can have a mixed effect. But, in general, increases in the porosity increase the 50% breakthrough time. However, the shallow slope in the points in Figure 4 indicates that the breakthrough time is not as sensitive to matrix porosity as it is to other parameters, such as the matrix partition coefficient.

1.5.7 Sensitivity to Fracture Saturation

In this sensitivity analysis, fracture saturation is changed to 0.01 and then from 0.1 to 1.0 in 10% increments. Although fracture saturation impacts the volume of water in fractures, which impacts the linear velocity of fluid moving through the system, fracture saturation has no impact on the 50% breakthrough time when varied between the base-case value of 0.0234 and full saturation. By rewriting the governing equation for transport in the fractures (Equation 1) in terms of Darcy velocity and saturation ($v = v_{Darcy}/sb$), it can also be seen that the effects of saturation and fracture aperture on the linear average velocity in the fracture are being offset by an equal impact of saturation and fracture aperture on the effective matrix diffusion term.

1.5.8 Sensitivity to Matrix Saturation

In this sensitivity analysis, matrix saturation is changed to 0.01 and then from 0.1 to 1.0 in 10% increments. In the GoldSim pipe pathway model, effective porosity of the matrix material is equated to the product of matrix porosity and the saturation. Therefore, the effect on transport of altering one of these parameters over the other is the same. The results in Figure 4 show that the 50% breakthrough times for changes in matrix porosity and saturation are similar.

1.5.9 Sensitivity to Dispersivity in the Fracture

In this sensitivity analysis, the base-case borehole dispersivity is changed from 0% to 500% of the base-case value. The dispersivity affects the movement of the solute in the vertical direction

ahead and behind the zone of highest concentration. The smaller values of dispersivity result in longer breakthrough times, but not significantly longer, as a value that is 90% of the base-case value only increases the 50% breakthrough time by about 1%. Doubling the dispersivity decreases the breakthrough time by 4%, and increasing the dispersivity by 500% results in an 18% decrease in the breakthrough time. Although the 50% breakthrough time arrives sooner for the higher dispersivity values, the 95% breakthrough time is delayed for higher dispersivity values. Increased dispersivity increases the spreading of the solute ahead of and behind the zone of highest concentration, requiring more time for 95% of the mass to reach the end of the pipe pathway.

1.6 SUMMARY

The technical basis for the delay of radionuclide transport due to matrix diffusion in the borehole is clarified by presenting the concept of matrix diffusion, including a presentation of the governing transport equations, verifying that the GoldSim pipe pathway solution for matrix diffusion is accurate, and by providing a sensitivity analysis that demonstrates the important parameters that delay transport in the borehole. In addition, the TSPA model configuration for the human intrusion borehole model has been summarized. The results of the sensitivity study demonstrate that the four most significant parameters governing the relative contribution of matrix diffusion over advection in the fractures are: (1) the applied flux rate in the fractures, (2) the sorption coefficients in the matrix, (3) the thickness of the matrix, and (4) the diffusive area between the fractures and the matrix.

The modeling approach of radionuclide transport through the human intrusion borehole is reasonable as shown by a sensitivity analysis of important parameters affecting the results. This analysis, with the assumptions and methodology of the transport, provide a transparent representation of the impact of the borehole on radionuclide transport.

2. COMMITMENTS TO NRC

None.

3. DESCRIPTION OF PROPOSED LA CHANGE

None.

4. REFERENCES

Moridis, G.J. 1998. *Semianalytical Solutions for Parameter Estimation In Diffusion Cell Experiments.* LBNL-41857. Berkeley, California: Earth Sciences Division, Lawrence Berkeley National Laboratory.

SNL (Sandia National Laboratories) 2007. *EBS Radionuclide Transport Abstraction.* ANL-WIS-PA-000001 REV 03. Las Vegas, Nevada: Sandia National Laboratories. ACC: DOC.20071004.0001

SNL 2008. *Total System Performance Assessment Model/Analysis for the License Application.* MDL-WIS-PA-000005 REV 00 AD 01. Las Vegas, Nevada: Sandia National Laboratories. ACC: DOC.20080312.0001

Sudicky, E.A. and Frind, E.O. 1982. "Contaminant Transport in Fractured Porous Media: Analytical Solutions for a System of Parallel Fractures." *Water Resources Research, 18,* (6), 1634-1642. Washington, D.C.: American Geophysical Union.

RAI Volume 3, Chapter 2.2.1.4.2, First Set, Number 3:

> Address the impact on overall performance of drilling through the perched water below the repository to the saturated zone, considering the volume and areal extent of the perched water and the potential effect on the transport of radionuclides within the unsaturated zone.
>
> Basis: DOE has included perched water in its TSPA as a feature that deflects radionuclide transport paths laterally to faults, then down to the saturated zone. The human intrusion scenario (i.e., borehole to the saturated zone) could result in a borehole penetrating the perched zone and thereby potentially affecting the pathway of radionuclides within the perched zone down to the saturated zone (i.e., radionuclides released from breached waste packages, which are transported to a perched zone, could subsequently enter the borehole and move down the borehole to the saturated zone). The staff needs this information to determine compliance with 10 CFR Part 63.322.

1. RESPONSE

The effect of open boreholes on repository performance, including the possible effect of a borehole passing through a perched water zone, has been considered in the analysis of features, events, and processes (FEPs) under FEP 1.1.01.01.0A. It was determined that this FEP was of low consequence and was therefore excluded from the performance assessment.

1.1 OCCURRENCE, AREAL EXTENT, AND VOLUME OF PERCHED WATER

Perched water in the Yucca Mountain region tends to occur when units with well-connected fracture porosity, such as in the Topopah Spring welded unit (TSw), overlie low-permeability or poorly fractured units such as the basal vitrophyre of the lower TSw, or the hydrothermally altered zeolitic Calico Hills unit (CHn). Figure 1 (SAR Figure 2.3.2-5) shows a cross section of these hydrogeologic units and a conceptualization of flow patterns near perched water bodies, indicating lateral fracture flow in the TSw above the perched zones. Although flow does occur through the fractures of the areally extensive basal vitrophyre, it is limited because the fractures are frequently filled with alteration products that tend to block flow .

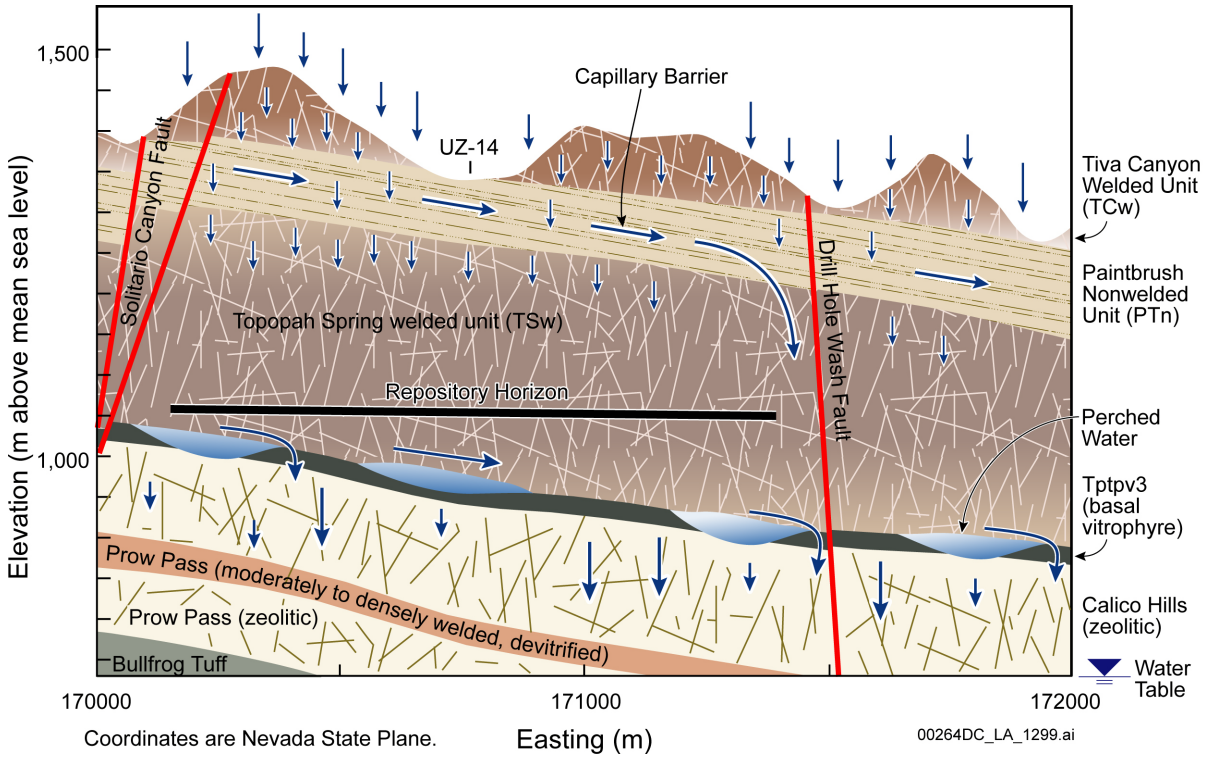

Source: SAR Figure 2.3.2-5.

Figure 1. Schematic Showing the Conceptualized Flow Processes near Perched Water Zones within a Typical West-East Cross Section of the Site-Scale Unsaturated Zone Flow Model Domain

Figure 2 shows the locations of the boreholes in the Yucca Mountain region that have encountered perched water, UZ-14, NRG-7a, SD-7, SD-9, SD-12, G-2, and WT-24 (SAR Section 2.3.2.2.2.4; SNL 2007, Section 6.2.2.2), which gives an indication of the areal extent of perched water relative to the repository footprint where the postulated human intrusion borehole may occur. The main perched water body surrounds UZ-14, SD-9, and NRG-7a under the northern part of the repository block. Pump tests demonstrated (Wu et al. 1999) that the upper permeable layer of the perched water zone is well connected hydraulically and exists primarily within the fractured, welded base of the lower TSw. The hydraulically well-connected zone is underlain by the low permeability basal vitrophyre and/or by the poorly fractured, low permeability zeolitic rocks of the CHn, which occur mostly in the northern part of the repository block.

Perched zones are insignificant beneath the southern part of the repository block where transport is dominated by matrix flow through the vitric unit of the CHn. Isolated perched water bodies at SD-7 and SD-12 are believed to be perched as a result of juxtaposition of units with different permeability at the Ghost Dance Fault. However, the perched water bodies have limited volume and extent (Wu et al. 1999) and do not contribute significantly to flow and transport beneath the repository.

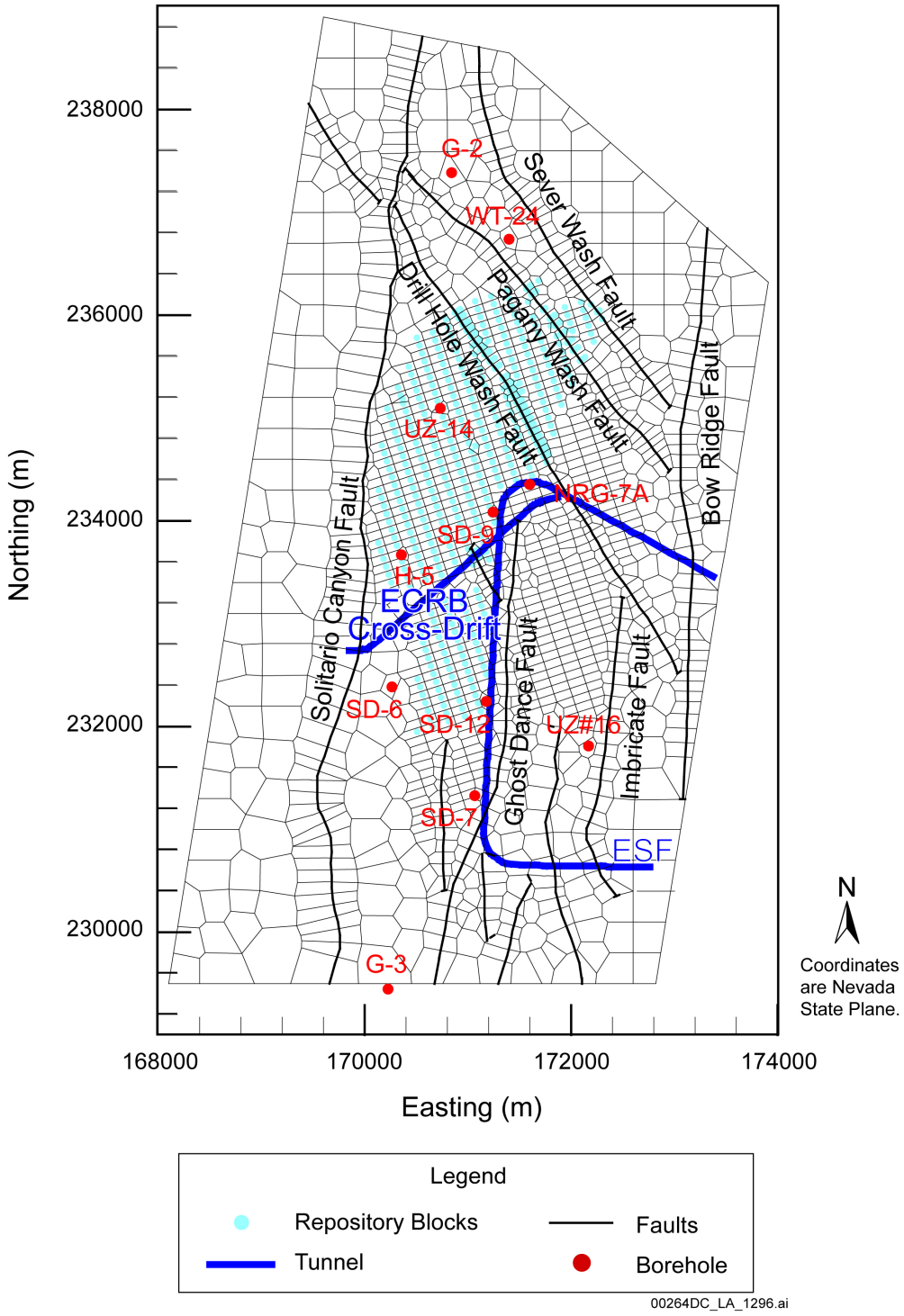

Source: SAR Figure 2.3.2-10.

NOTE: Perched water has been observed in UZ-14, NRG-7a, SD-7, SD-9, SD-12, G-2, and WT-24.

Figure 2. Location of Select Boreholes on Plan View of the Three-Dimensional Site-Scale Unsaturated Zone Flow Model Domain

Estimates of water volumes for the perched zone identified at boreholes UZ-14, SD-9, and NRG-7a are based on numerical simulations calibrated to results of several pumping tests conducted at UZ-14 (Wu et al. 1999, Section 5, p. 178). Wu et al. (1999) estimate the formation volume of the perched zone to be on the order of 5.0×10^7 m^3 (or equivalent to a cylinder with a radius equal to 900 m and a thickness equal to 20 m). The perched water volume is then equal to 6.5×10^5 m^3, determined by multiplying the formation volume by the porosity (0.013) of the lower TSw unit (SNL 2008b, Section 6.5.7, Table 6-14, Unit TSwF7). These volume estimates are for the hydraulically connected, higher permeability parts of this perched zone located in the lower fractured portion of the TSw. A larger perched water volume may be present in the underlying zeolitic CHn but is not hydraulically significant (i.e., will not flow into a human intrusion borehole) because of the high capillarity associated with these tight zeolitic rocks.

Based on the above estimate of an equivalent circular area for the perched body, the storage capacity of the perched zones is relatively small in comparison with the volume of water moving through the unsaturated zone. Specifically, based on the calculated radius of 900 m, the circular area would be about 2.5×10^6 m^2. Using this area, and assuming a Darcy flux of about 20 mm/yr in the glacial-transition climate (SAR Table 2.3.2-14, gt_30), a bounding estimate for the residence time within the perched zone would be about 13 years, if it is assumed to be a single porosity medium through which flow is vertical. Thus, its capacity for storage of radionuclide mass, and consequent maximum contribution to overall vertical flux of radionuclide mass, would be quite small over the time frames being considered for repository performance. However, any potential drainage of these perched zones by a single degraded human intrusion borehole would only occur over a limited area surrounding the borehole. The effect of limited drainage of the perched zones into fast pathways, whether they are boreholes or faults, is supported by the current estimated age of the pore water in the perched zones, which ranges from approximately 3,300 to 11,000 years (SAR Section 2.3.2.3.4) based on geochemical analysis of ^{14}C ages in the perched water bodies. Thus, even though perched water bodies are adjacent to fault zones, isotopic dating indicates little interaction between them. The same behavior would be expected for the high permeability pathway that remains after natural degradation processes have modified the human intrusion borehole.

The effects of expected future wetter climates will increase infiltration above the repository and will likely lead to an increase in the extent and volume of these perched zones. However, the intrusion of a perched water body, regardless of extent, would have a negligible impact on flow through the unsaturated zone.

1.2 FLOW AND TRANSPORT FROM REPOSITORY TO PERCHED WATER

Just below the repository but above the perched water, the gently eastward dipping TSw has low porosity and widespread fracturing typical of densely welded tuffs, which results in fracture-dominated advective-dispersive transport (Figure 1). The strongly altered northern part of the CHn unit, composed of zeolites and clays with low permeability and poorly developed, sparsely connected fractures, results in a low permeability layer. Because of the low permeability, water flux to the CHn unit and just above the perched zone may be diverted laterally, down-dip to the east towards the faults, which act as main pathways for fast flow and transport in the unsaturated zone. A human intrusion borehole through the perched zone may act as a high permeability fast

flow pathway to the water table, capturing the lateral flow above the perched zone, similar to fractures and faults.

The principal difference between the high-permeability pathways presented by fracture networks in the TSw and the borehole is that the area of the borehole available to intercept lateral flow is much smaller than the area associated with fractures. The exclusion argument for FEP 1.1.01.01.0A (SNL 2008a) includes calculations of the combined cylindrical area of 15 open boreholes with average borehole diameters estimated to be 1 m, and depths greater than 1,000 ft. The combined cylindrical area of the 15 boreholes is estimated to be equal to 15π m^2/m (47 m^2/m), considerably greater than an 8-inch (20.3 cm) diameter single borehole from a human intrusion. Both permeabilities are insignificant compared to the minimum fracture area per unit depth of about 5×10^5 m^2/m for the unsaturated zone fracture network underlying the repository (SNL 2008a, FEP 1.1.01.01.0A). Therefore, the introduction of the human intrusion borehole in this zone would not significantly increase the vertical flow and advective transport of radionuclides from the repository to the perched zone, in comparison to the flow expected within the rock mass fracture network.

1.3 FLOW AND TRANSPORT FROM PERCHED WATER TO WATER TABLE

The primary perched water zones are beneath the northern part of the repository footprint above the low permeability units of the TSw basal vitrophyre and the zeolitic CHn. These same low permeability units not only result in perched water but also in down-dip lateral flow to the fault zones. Flow through these fault zones is rapid, resulting in short travel times from the perched water bodies to the water table in the northern part of the repository. Because of this already fast travel time, the penetration of the perched zones by a fast-pathway human intrusion borehole (SAR Section 2.4.3.3.5.1) would not result in a significant change in the transport characteristics of the unsaturated zone beneath the northern portion of the repository. Also, perched zones are of limited extent beneath the southern regions of the repository, so a human intrusion borehole in the southern region would not have a significant impact on perched zones.

The large impact of faults below the repository is apparent when comparing the water flux through the faults with the water flux through the fractures of non-fault zones and through the host rock matrix at two horizons: the repository horizon and the water table. At the repository horizon, only about 1% of the total water flux is in faults, but this increases to about 30% at the water table, suggesting that a large portion of the water flow is diverted to the faults (Table 1).

Table 1. Comparison of Water Flux Distribution between Fractures of Non-Fault Zones, Matrix, and Faults at the Repository and Water Table Horizons for the Four Post-10,000-Year Flow Fields

Simulation Designation	Flux at Repository Horizon[a] (%)			Flux at Water Table[b] (%)		
	Fracture	Matrix	Fault	Fracture	Matrix	Fault
pkd_q1	95.79	3.32	0.89	56.95	19.96	23.09
pkd_q2	96.88	1.84	1.29	50.42	16.87	32.70
pkd_q3	97.09	1.49	1.42	47.89	15.10	37.01
pkd_q4	97.58	1.37	1.05	58.55	6.26	35.18

Source: [a]SNL 2007, Table 6.6-2; [b]SNL 2007, Table 6.6-3.

At the repository horizon, only approximately 2% of the total water flux is in the matrix, but this increases to about 15% by the water table. This is explained by the presence of hydrogeologic units with significant matrix flow (such as the nonzeolitic CHn and the nonzeolitic Crater Flat undifferentiated), which occur in the southern half of the repository, where perched zones are limited.

The results in Table 1 are further supported by Figure 3 (SAR Figure 2.3.8-37), which compares particle release locations at the repository horizon (Figure 3(a)) and the particle exit locations at the water table (Figure 3(b)). The majority of particles in the northern part of the repository travel through the faults, whereas far more particles are transported through the matrix in the south. Transport through the faults, assuming a conservative species without decay or matrix diffusion, is generally less than 100 years (Figure 3(c); also see FEP 1.1.01.01.0A). Thus, a fast pathway through a human intrusion borehole would have little influence on the already existing fast transport times below the perched water bodies. (Note: Although Figure 3 displays results calculated using the glacial-transition, 10th percentile infiltration rates (SAR Table 2.3.2-14), it is assumed here that using the equivalent or higher post-10,000-year infiltration rates (SAR Table 2.3.2-15) would likely result in comparable or faster travel times associated with flow in the faults to the water table.)

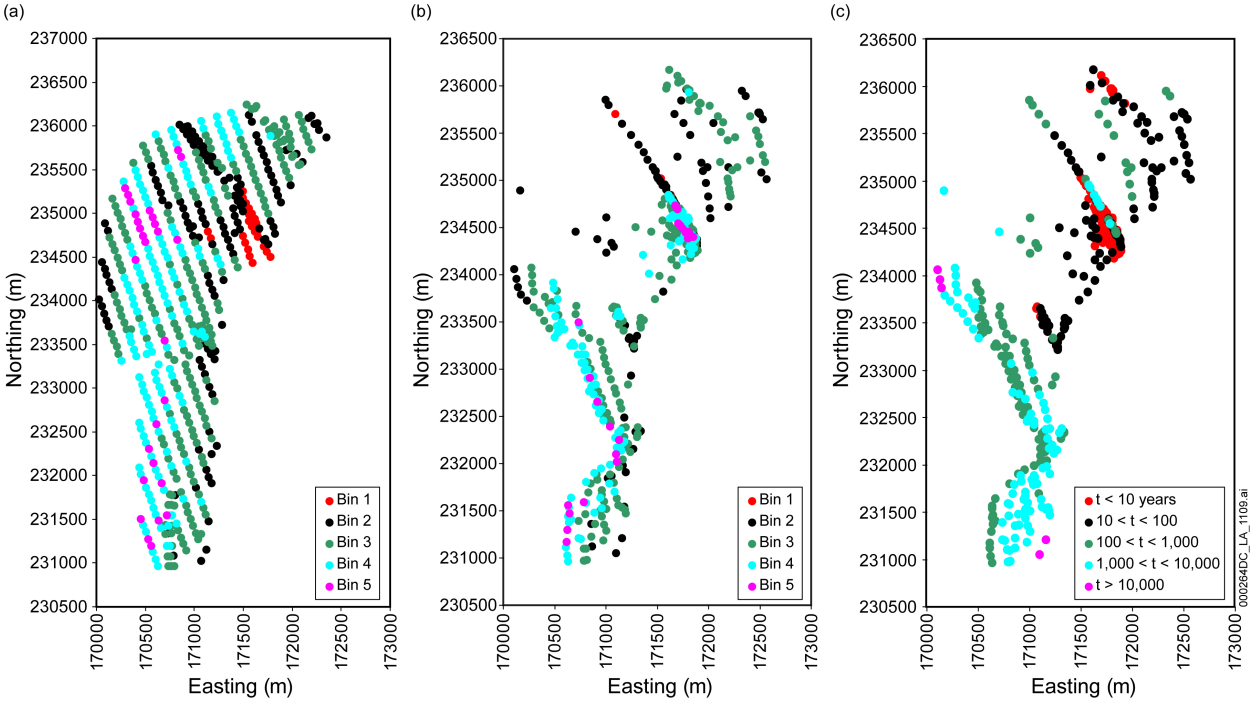

NOTE: For this flow field, upper percolation rates for each bin are: Bin 1 = 0.82, Bin 2 = 4.55, Bin 3 = 14.06, Bin 4 = 26.16, and Bin 5 = 36.19 mm/yr. Panel (c) shows the exit locations from the unsaturated zone at the water table plotted with mean travel time of a conservative species without decay or matrix diffusion.

Source: SAR Figure 2.3.8-37.

Figure 3. Comparison of (a) Particle Release Locations and (b) Exit Locations in Terms of Percolation Bin Assignment or (c) Mean Travel Time for Flow Fields Developed Using the Glacial-Transition, 10th Percentile Infiltration Map

Finally, transport below the perched water bodies involves relatively less interaction with the rock matrix compared with transport through the Topopah Spring (TSw) rock units (above the perched bodies); hence transport from perched water levels to the water table, dominated by transport through faults, is relatively fast compared with transport from the repository to the perched water (SNL 2008a, FEP 1.1.01.01.0A). Therefore, any possible reduction in travel time associated with radionuclide transport through borehole pathways (rather than fault pathways) below perched water bodies would have a negligible effect on performance because travel times through the northern part of the unsaturated zone are dominated by transport in the TSw above the perched zones.

1.4 SUMMARY

Boreholes inadvertently drilled from the ground surface down to the water table are not expected to produce a significant enhanced pathway for flow and radionuclide transport between the repository and perched water or from the perched water to the water table, because the fracture and fault flow in the unsaturated zone is much greater than in these boreholes. Thus, there would be a negligible impact on performance in the human intrusion scenario from drilling a single borehole through a perched zone. Specifically, the storage capacity of the perched zones is relatively small in comparison with the volume of water moving through the unsaturated zone; the area of the intrusion borehole is negligible in comparison to fracture area when considering lateral, down-dip flow through the TSw unit above the perched water bodies; and the potential reduction in travel time from the perched water body to the water table, arising from the borehole intrusion, is inconsequential because fault flow already results in a short travel time for the lower portion of the unsaturated zone.

2. COMMITMENTS TO NRC

None.

3. DESCRIPTION OF PROPOSED LA CHANGE

None.

4. REFERENCES

SNL (Sandia National Laboratories) 2007. *UZ Flow Models and Submodels.* MDL-NBS-HS-000006 REV 03 AD 01. Las Vegas, Nevada: Sandia National Laboratories. ACC: DOC.20080108.0003.

SNL 2008a. *Features, Events, and Processes for the Total System Performance Assessment: Analyses*. ANL-WIS-MD-000027 REV 00. Las Vegas, Nevada: Sandia National Laboratories. ACC: DOC.20080307.0003.

SNL 2008b. *Particle Tracking Model and Abstraction of Transport Processes.* MDL-NBS-HS-000020 REV 02 AD 02. Las Vegas, Nevada: Sandia National Laboratories. ACC: DOC.20080129.0008

Wu, Y.S.; Ritcey, A.C.; and Bodvarsson, G.S. 1999. "A Modeling Study of Perched Water Phenomena in the Unsaturated Zone at Yucca Mountain." *Journal of Contaminant Hydrology, 38,* (1-3), 157-184. New York, New York: Elsevier.